

methods. The measurements relevant to this work and their corresponding effective measurement resolution are listed in Table 1.

2.1.1 Continuous flow chemical measurements

The Desert Research Institute (DRI) Ultra Trace Chemistry Laboratory makes continuous and simultaneous measurement with high depth resolution for many chemical elements, black carbon, dust and water isotopes in ice cores using a black carbon (BC) and trace element continuous flow analysis (BC-TE-CFA) system (McConnell, 2002, 2010; McConnell et al., 2007; McConnell and Edwards, 2008; McConnell et al., 2014; Pasteris et al., 2014a, b). With BC-TE-CFA analyses, longitudinal samples of ice core (cross-sectional area of 3.3 cm × 3.3 cm and ~ 100 cm long) were melted sequentially with the meltwater stream split into three regions. Meltwater from the innermost ring is used for inductively coupled plasma mass spectrometry (ICP-MS) using two parallel instruments (Element 2; Thermo Scientific), and for BC mass and particle size distribution measurements using a laser-based instrument (SP2; Droplet Measurement Technologies) (Schwarz et al., 2006) coupled to an ultrasonic nebulizer (A5000T; Cetac) (Bisiaux et al., 2012; McConnell et al., 2007). Meltwater from the middle ring is used for traditional continuous flow measurements of nitrate, liquid conductivity, ammonium, and pH (Pasteris et al., 2014b, 2012). Analyses of aerosols are complemented by addition of a laser-based particle counter (Abakus; Klotz) into the melt stream that quantifies size-resolved aerosol mass (Ruth et al., 2003). Measurements used in this study are from four analysis campaigns taking place between 2008–2014, with small additions and improvements applied to the analytical setup over this timespan. Modifications, for example, resulted in improved resolution of the insoluble particle concentration data below 2711 m (> 28 kaBP) that allowed a joint annual-layer interpretation in combination with the ECM record. About 15 % of the core at regularly spaced intervals was rerun using duplicate samples of ice, to provide a check on issues that might adversely influence the data quality over the six-year period that measurements were made.

The WAIS Divide deep ice core WD2014 chronology

M. Sigl et al.

Title Page

Abstract

Introduction

Conclusions

References

Tables

Figures



Back

Close

Full Screen / Esc

Printer-friendly Version

Interactive Discussion



At ice melt rates of approximately 5 cm min^{-1} , the system achieved a depth resolution for most analytes of approximately 1–2 cm in ice and $> 2 \text{ cm}$ in low-density firn due to larger signal dispersion. High sampling resolution (in combination with high annual snowfall rates) permits detection of annual cycles in impurity data (Table 1; Fig. 1), a prerequisite for precise annual dating of ice core records (Rasmussen et al., 2006; Sigl et al., 2013). The BC-TE-CFA system is well suited for ice samples that are long continuous pieces. Depending on how the instruments were configured, the annual layers had to be thicker than 2.5 cm (dust; used below 2711 m depth, see Fig. 1) or 7 cm (all other parameters) to be confidently identified.

2.1.2 Discrete chemical measurements

Between about 577 and 1300 m depth, the ice was brittle due to stress in the ice-air bubble matrix (the brittle ice zone), and the quality of the ice core was reduced. Ice-core sample quality was rated poorest between 1000 and 1100 m depth corresponding to an age interval of 4.3–4.9 kaBP (Souney et al., 2014). Where sample quality permitted, measurements of trace chemical impurities were performed online with a continuous flow analysis system with ion chromatography detection (CFA-IC) at the Trace Chemistry Ice Core Laboratory at South Dakota State University (Cole-Dai et al., 2006). This technique consists of an ice core melter linked to a group of eight ion chromatographs (four Dionex DX-600 for anion detection, four Dionex ICS-1500 for cation detection, respectively). Longitudinal samples of ice core (cross-sectional area of $3.5 \text{ cm} \times 3.5 \text{ cm}$) were melted sequentially at an ice melt rate of about 2.4 cm min^{-1} with the meltwater stream from the inner zone feeding the IC instruments. This analytical technique has previously been applied to various ice cores from Antarctica and Greenland achieving reproducible results in agreement with discrete measurements (Cole-Dai et al., 2009; Cole-Dai et al., 2013; Ferris et al., 2011; Jiang et al., 2012). The CFA-IC setup used for the WD analysis provided major-ion analysis and can resolve annual layers in the brittle ice zone of WD (Table 1; Fig. 1). Where sample quality did not permit use of the online

CPD

11, 3425–3474, 2015

The WAIS Divide deep ice core WD2014 chronology

M. Sigl et al.

Title Page

Abstract

Introduction

Conclusions

References

Tables

Figures



Back

Close

Full Screen / Esc

Printer-friendly Version

Interactive Discussion



continuous technique (38% of the depth interval), discrete samples were individually decontaminated and analysed using traditional IC techniques (Cole-Dai et al., 2000).

2.1.3 Electrical measurements

Seasonal variations of the ice chemistry influence the electrical conductivity of the ice, which allow electrical measurements to detect annual layering (Hammer, 1980; Taylor et al., 1997). Three types of electrical measurements were employed. In the brittle ice, dielectric profiling (DEP) was used because it is insensitive to close-fitting fractures and the low spatial resolution was not a concern because the annual layers were thicker than 15 cm. For the remainder of the core, two types of electrical conductivity measurements were used, alternating current (AC-ECM) and direct current (DC-ECM). The AC-ECM is primarily controlled by the acidity but also responds to other ions (Moore et al., 1992), and it can identify annual layers thicker than 2 cm. The DC-ECM is controlled by the acidity of the ice. The data quality of the DC-ECM was improved by making multiple measurements along the core, which made it possible to avoid the adverse influence of many fractures in the core. DC-ECM has the highest spatial resolution of all the measurements described here and can identify annual layers that are thicker than 1 cm (Taylor et al., 1997).

2.1.4 ^{10}Be measurements

^{10}Be concentrations for the WAIS Divide ice core for Sects. 0–577 and 1191–2453 m depth were measured at UC Berkeley's Space Sciences Laboratory and Purdue's PRIME Laboratory (Woodruff et al., 2013). Sampling resolution varied from 1.9 to 4.2 m, but samples typically represented continuous ice core sections of 3 m length. The time resolution of each sample ranged from 10 to 30 years for the past 12 ka BP. $^{10}\text{Be}/^9\text{Be}$ ratios of all samples were measured by accelerator mass spectrometry (AMS) and normalized to a ^{10}Be AMS standard (Nishiizumi et al., 2007). ^{10}Be concentrations in the ice and the ^{14}C content in tree rings are both influenced by the varying

The WAIS Divide deep ice core WD2014 chronology

M. Sigl et al.

Title Page

Abstract

Introduction

Conclusions

References

Tables

Figures



Back

Close

Full Screen / Esc

Printer-friendly Version

Interactive Discussion



flux of cosmic rays, hence ^{10}Be measurements provide a link between the ice-core and tree-ring chronologies (Muscheler et al., 2014).

2.2 Seasonality in aerosol deposition

Most of the aerosol records from WAIS Divide show strong seasonal variations due to seasonality in aerosol source strength and transport efficiency, and these seasonal signals can be used to detect annual layers (Banta et al., 2008; Sigl et al., 2013). For example, Southern Hemisphere forest and grass fires usually peak during a confined burning season following the meteorological dry period driven by seasonal insolation changes (Bowman et al., 2009; Schultz et al., 2008; van der Werf et al., 2010), and aerosols emitted by these fires (e.g., black carbon) get transported and deposited on the Antarctic ice sheet (Bisiaux et al., 2012) with peak concentrations in austral autumn.

A typical annual layer at WAIS Divide is characterized by a concentration maximum of biomass burning tracers (e.g., BC, NH_4^+) in austral autumn, maximum from sea-salt deposition (e.g., Na, Cl) during austral winter, and a maximum of marine biogenic aerosol emission tracers (e.g., S, Br) in late austral summer (Fig. 2). Dominant sources, absolute concentrations, and relative timing of deposition of the various aerosols are, however, not stationary through time (Fischer et al., 2007; Wolff et al., 2010). Concentrations and fluxes of Ca, Mg, and insoluble particles, for example, are low during the Holocene and are dominated by a sea-salt source (indicated by co-deposited Na and Cl), whereas during the Antarctic Cold Reversal (ACR) (Fig. 2) and during the glacial (Fig. 3) concentrations and fluxes at WAIS Divide are often higher by an order of magnitude and dominated by continental dust sources (as indicated by co-deposited dust tracers such as V, Cr, and Ce). In contrast, BC concentrations at WAIS Divide are driven by a constant single source – natural forest and savannah fires in the Southern Hemisphere – but Holocene concentrations are more than twice as large as during the late glacial period (Fig. 2).

CPD

11, 3425–3474, 2015

The WAIS Divide deep ice core WD2014 chronology

M. Sigl et al.

Title Page

Abstract

Introduction

Conclusions

References

Tables

Figures



Back

Close

Full Screen / Esc

Printer-friendly Version

Interactive Discussion



Section 577–1300 m (2345–6009 aBP; brittle ice zone)

For the brittle ice, where drilling fluids may have penetrated the ice through internal cracks, it is more difficult to obtain undisturbed and uncontaminated high-resolution chemistry records. The fractures precluded using the DRI continuous flow chemistry system and measurements were instead made at South Dakota State University. Ice with many fractures was measured with discrete samples while ice with few fractures was measured using continuous flow analysis (Cole-Dai et al., 2006).

Manual interpretation of annual layers was performed with non-sea-salt sulfate (nssSO_4^{2-}) as the primary parameter, and using Na^+ and NO_3^- as secondary parameters (Fig. 4). When establishing WDC06A-7 (WAIS Divide Project Members, 2013), the independent DEP data set was used, with the annual layers initially identified with the selection curve algorithm (McGwire et al., 2011) subsequently manually verified or rejected. An initial reconciliation by one interpreter of the multi-parameter chemistry and DEP was performed. This interpretation was re-examined once the tendency for the ECM to overcount was discovered by comparison to the multi-parameter measurements (WAIS Divide Project Members, 2013) and after the comparison of ^{10}Be and ^{14}C showed the interpretation to have more years than the tree ring timescale (see Sect. 3.1). A consensus decision was then obtained by two investigators using both data sets. The StratiCounter algorithm was not run for this interval. This is the first time annual layers have been identified in chemistry data through the brittle ice zone, which occurs in all deep ice cores.

Section 1300–1940 m (6009–11 362 aBP)

Below 1300 m core quality was excellent and we used records obtained by the DRI continuous flow system. The average layer thickness remained above 10 cm and the annual cycles were well resolved in all parameters (Fig. 5). The primary aerosol records used were BC, nssS, Na, and nssS/Na. The aerosols were interpreted both manually and with the StratiCounter algorithm. Any differences between the manual, Strati-

The WAIS Divide deep ice core WD2014 chronology

M. Sigl et al.

Title Page

Abstract

Introduction

Conclusions

References

Tables

Figures



Back

Close

Full Screen / Esc

Printer-friendly Version

Interactive Discussion



Counter, and ECM interpretations were investigated by three interpreters and a consensus was reached.

Section 1940–2020 m (11 362–12 146 aBP)

For this interval, a multi-parameter (aerosol and ECM) interpretation had already been performed for the WDC06A-7 timescale to confirm the observed sharp rise in annual layer thickness (WAIS Divide Project Members, 2013). To estimate the reliability of the layer counting, the StratiCounter algorithm was also run on this interval using the multi-parameter aerosol data set (Table 2) which re-confirmed this rise in layer thicknesses. The WD2014 interpretation is unchanged from WDC06A-7 since it was based on the larger data set of both ECM and aerosol records.

Section 2020–2300 (12 147–15 302)

The average annual-layer thickness during this interval was less than 10 cm (Fig. 8), making it more difficult to confidently identify all annual layers using the DRI continuous aerosol data (Fig. 6). The ECM retained sufficient measurement resolution. Thus, the interpretation relied upon the ECM records more than at shallower depths. The StratiCounter algorithm was run to 2274 m depth, but since the StratiCounter interpretation was not used as much in the deeper part, we did not extend use of the algorithm to 2300 m.

Section 2300–2711 m (15 302–26 872 aBP)

In this depth interval, the aerosol records did not have sufficient depth resolution for reliable identification of the annual signal so the annual-layer interpretation is based solely on ECM data. The interpretation was not changed from WDC06A-7 because (a) the ECM interpretation agreed well with the consensus interpretation between 2020 and 2300 m (Table 2), (b) it agreed well with the dust data between 2711 and 2800 m (Table 2), and (c) the age comparison in the glacial period (Sect. 3.2) showed no sig-

The WAIS Divide deep ice core WD2014 chronology

M. Sigl et al.

Title Page

Abstract

Introduction

Conclusions

References

Tables

Figures



Back

Close

Full Screen / Esc

Printer-friendly Version

Interactive Discussion



The WAIS Divide deep ice core WD2014 chronology

M. Sigl et al.

Title Page

Abstract

Introduction

Conclusions

References

Tables

Figures



Back

Close

Full Screen / Esc

Printer-friendly Version

Interactive Discussion



nificant bias. The only period of reinterpretation is for 2421.75 and 2427.25 m depth corresponding to a period of enhanced acid deposition at WAIS-Divide that forms a distinctive horizon and prominent radar reflector across West Antarctica (Hammer et al., 1997; Jacobel and Welch, 2005). During this approximately 200 year long deposition event, the annual-layer dating was based on dust particle concentrations. The additional measurements were made using a second stick from the main core and a modified analytical setup with increased measurement resolution of the *Abakus* particle counter. Annual layers in the dust were identified using the automated interpretation from the selection curve algorithm (McGwire et al., 2011) with manual adjustments that included the ECM data during periods without volcanic acid deposition.

Section 2711–2800 m (26 872–29 460 a BP)

In this section of the core, the DRI continuous analytical system was modified to increase the resolution of the particle counter measurements. This allowed insoluble particle concentration data to also be used as an indicator of annual layers between 2711 and 2800 m depth. These data were interpreted with the StratiCounter algorithm, and compared to the interpretation of the ECM based on the selection curve algorithm. The final timescale was mostly found by adopting the previous interpretation of the ECM data, but the particle record with the StratiCounter layer interpretation was used to make manual adjustments when the ECM layer signal was ambiguous.

Section 2800–2850 m (29 460–31 247 a BP)

The annual-layer interpretation was extended using the ECM data past the 2800 m stopping depth of WDC06A-7. Particle concentration data was also interpreted with the StratiCounter algorithm, but the results were deemed unreliable with too few layers being identified, likely due to too low resolution of the record. Layer interpretation in the ECM data below 2850 m became increasingly difficult. This difficulty in interpreting the annual cycles appears to be driven by a lack of amplitude in the annual cycle as well

the black carbon recorded the annual signal because it is only influenced by biomass burning on a hemispheric scale.

The uncertainty associated with the ability to correctly interpret the annual layers occurs because a small percentage of the features in the records can be interpreted in several ways. To overcome this we used records indicative of multiple aspects of the climate system (dust, black carbon from biomass burning, nssS-Na, electrical conductivity), and we used multiple interpretation methods (machine assisted interpretation and multiple manual interpreters). The vast majority of annual layers were clearly visible in at least one data set, but in some cases multiple interpretations were possible.

It is not possible to rigorously calculate the uncertainty of the depth–age relationship for the WAIS Divide core. Although there are multiple parameters that express the annual signal, and multiple methods to interpret the annual signal, they all rely on an ice sample from the same 12 cm diameter cylinder from the ice sheet. We have higher confidence in depth intervals where all layer interpretations were consistent and layers appeared well resolved by the measurements. We have lower confidence deeper in the core where ice flow has thinned the layers to such extent that they are approaching the ability of the measurements to resolve them. For example, in the upper part of the ice core, all aerosol records showed clear peaks and troughs between neighbouring maxima (Figs. 4 and 5); in the lower part of the core, layer boundaries were in some aerosol records (e.g., nssS, Na) occasionally only recognizable by small inflections in the concentration data (Fig. 6).

For the Greenland GICC05 timescale, ambiguous layers were identified and used to estimate uncertainty in the annual-layer interpretation. Each “uncertain” annual layer was counted as 0.5 ± 0.5 years, and the half-year uncertainties were summed to determine a “maximum counting error” estimated to represent a 2σ age uncertainty (Andersen et al., 2006; Rasmussen et al., 2006; Svensson et al., 2006). We did not take this approach because: (1) it assumes the ice core records the seasonal variations without any bias towards recording too many or too few layers, (2) it assumes the interpretation errors are equally split between too many and too few years, and (3) classifying

The WAIS Divide
deep ice core
WD2014 chronology

M. Sigl et al.

Title Page

Abstract

Introduction

Conclusions

References

Tables

Figures



Back

Close

Full Screen / Esc

Printer-friendly Version

Interactive Discussion



The WAIS Divide deep ice core WD2014 chronology

M. Sigl et al.

Title Page

Abstract

Introduction

Conclusions

References

Tables

Figures



Back

Close

Full Screen / Esc

Printer-friendly Version

Interactive Discussion



interval. From 2020 to 2274 m, the consensus decision found 2834 years, which was 0.3 % less than the manual aerosol interpretation and 0.7 % less than the ECM interpretation. The StratiCounter interpretation found a much smaller number of 2645 years (7 % less). At these depths, the annual layer thickness is near the resolution limit of the aerosol measurements and thin years were not well resolved. The StratiCounter algorithm seemed to miss the small expression of these layers.

Between 2200 and 2300 m depth, the total number of annual layers based on manual interpretation from aerosols and ECM agreed within a few years. The aerosol layer interpretation became increasingly difficult, and we stopped interpreting the multi-parameter aerosol records at 2300 m depth.

For the intervals from 2300 to 2711 m, and between 2800–2850 m, where only the ECM data resolve annual layers, there is no way to test the interpretation repeatability. In sections where only ECM data was available for dating, the duration of volcanic events was dated under the assumption of constant annual-layer thickness, thereby resulting in less confidence in the layer interpretation.

Between 2711–2800 m, improved resolution of the particle concentration data allowed a comparison between layer counts based on the ECM and particle concentration records, respectively. StratiCounter layer counts based on the particle concentration data identified 2649 layers, which was 2 % more than the ECM-based counts.

3 Comparison to other time scales

The interpretation repeatability in Table 2 and described above is not a measurement of the accuracy of the chronology over long time periods, since over longer sections, the layer interpretation uncertainties are expected to partially cancel out (e.g. Ras-mussen et al., 2006). To assess the accuracy of WD2014 we need to compare it to other chronologies with high accuracy and defined uncertainty. We have selected the tree-ring based radiocarbon calibration chronology (Reimer et al., 2013; Friedrich et al., 2004) and the Hulu cave chronology (Edwards et al., 2015). The tree ring chronology

East Asian monsoon. The changes in these three parameters are expected to be near-synchronous (Buizert et al., 2015; Rosen et al., 2014; Svensson et al., 2008, 2006).

Methane synchronization (Buizert et al., 2015) provides a means to independently assess the accuracy of the annual-layer counted WD2014 chronology because some speleothem records, e.g., the Hulu cave in China (Edwards et al., 2015; Wang et al., 2001), have very precise age scales (based on U/Th dating). The ice-age gas-age difference (Δ age) is relatively small for WD ($\leq 525 \pm 120$ years throughout the WAIS Divide core) because of the high annual snowfall rates at the site. The uncertainty of the lag of atmospheric CH_4 behind Greenland $\delta^{18}\text{O}$ is on the order of a few decades (Huber et al., 2006; Baumgartner et al., 2014; Rosen et al., 2014), and the total gas-age uncertainty (for ages older than approximately 11 ka BP) is dominated by the cumulative annual-layer interpretation uncertainty (Table 4). The methodology and results of the methane synchronization are described in detail in the companion paper addressing the deeper part of the WD2014 chronology (Buizert et al., 2015).

Comparing the onset of DO 3, DO 4 and DO 5.1 as determined from the WD2014 gas-age scale and Hulu cave shows that WD2014 is consistently younger than Hulu. The maximum age difference between WD2014 and Hulu is 167 years (0.6 % of the age) for the onset of DO 3 (Table 3). The WD2014 ages agree with the Hulu ages to within the combined Hulu age uncertainty and the WAIS Divide gas-age uncertainty (Buizert et al., 2015). The age difference between WD2014 and Hulu is much less than the cumulative uncertainty in identifying annual layers in WD2014.

3.3 Age accuracy

As described above, Table 3 shows the comparison of WD2014 to these records at times when we are able to confidently make a stratigraphic link to either the tree ring ^{14}C record or the Hulu cave $\delta^{18}\text{O}$ record. The age confidence is more difficult to determine when there are no age comparisons. This encompasses large portions of the timescale: the brittle ice zone (2.4 ka to 5.5 ka BP) and the glacial–interglacial transition to the last glacial maximum (11 ka to 27 ka BP). Considering the interpretation repeata-

The WAIS Divide deep ice core WD2014 chronology

M. Sigl et al.

Title Page

Abstract

Introduction

Conclusions

References

Tables

Figures



Back

Close

Full Screen / Esc

Printer-friendly Version

Interactive Discussion



The WAIS Divide deep ice core WD2014 chronology

M. Sigl et al.

Title Page

Abstract

Introduction

Conclusions

References

Tables

Figures



Back

Close

Full Screen / Esc

Printer-friendly Version

Interactive Discussion



bility (Table 2) and the comparison to the tree-ring chronology (Fig. 9), we recommend considering the ages in WD2014 to be accurate to better than 0.5 % in the Holocene (to 11 ka). Without any comparisons for the next 16 000 year interval, estimating the age accuracy is difficult. The comparisons with the Hulu Cave chronology indicate that the oldest part of the WD2014 annual timescale is accurate to within 1 % of the age. We suggest using a 1 % age confidence for the timescale older than 14.5 ka. Between 11 and 14.5 ka, the age confidence is likely better than 1 % because there has been a limited number of years since 11 ka to accumulate uncertainty. Therefore, we linearly increase the age confidence from ± 55 years at 11 ka to ± 145 years at 14.5 ka.

We recognize that is not a rigorous determination of uncertainty; however, it is the best that can be done with the information that is available now or in the foreseeable future. We also note that the uncertainty in the time between two climate events is not the difference between the age accuracy of the two climate events. The age accuracy is better than the cumulative interpretation repeatability because errors in identification of the annual layers tend to cancel out. The uncertainty of the time between two climate events is better estimated by the interpretation repeatability.

3.4 Comparison to the Greenland ice core chronology GICC05

Here we summarize the observed age differences as derived from the methane synchronization to the GICC05 $\delta^{18}\text{O}$ chronology for rapid climate transitions within the annual-layer counted part of the WD2014 chronology (Table 4). The abrupt climate changes observed in the NGRIP $\delta^{18}\text{O}$ record and leading to global methane rise (Baumgartner et al., 2014; Buizert et al., 2015) are clearly expressed during the onset of the Younger Dryas/Holocene warming, Bølling/Allerød warming, and DO 3, DO 4, and DO 5.1 while the termination of the inter-stadials appears more gradually (Buizert et al., 2015; NGRIP-Project-Members, 2004; Wang et al., 2001).

The absolute calendar ages for the Bølling/Allerød warming and the Preboreal warming are slightly younger on WD2014 than GICC05 (Fig. 10) but agree within the GICC05 uncertainty. A dating correction of approximately 70 years for GICC05 for the early

Holocene has recently been independently proposed based on synchronizing the GRIP ¹⁰Be record to the Intcal13 radiocarbon chronology (Muscheler et al., 2014) and by matching of distinctive tephra horizons between Greenland ice cores and radiocarbon-dated lake sediments from Kråkenes Lake, Norway (Lohne et al., 2013, 2014). WD2014 is older than GICC05 at DO 3 by 52 years at DO 4 by 198 years and by 24 years at DO 5.1 (Fig. 10; Table 4). The terminations of the DO events are all older on WD2014 than GICC05 by 49 years at DO3, 174 years at DO4, and 72 years at DO 5.1.

We can also compare the duration of intervals although this is more challenging due to uncertainties in the feature matching; the Δ age and feature matching uncertainties are on the order of 100 years during the DO events. However, the Δ age uncertainty is likely biased in the same way for events at similar times (i.e. if the temperature reconstruction is too cold for DO3 it is likely too cold for DO4 as well leading to a Δ age that is too large for both events) such that much of it may cancel when calculating the duration. Therefore, while we calculate the duration differences in Table 5, we recognize that more precise matching of the timescales must be done (e.g., using volcanic synchronization) before definitive differences between the timescales can be ascertained.

A potential concern of the WD2014 timescale is that annual layers might be systematically missed near the end of the timescale due to small layer thicknesses and decreasing amplitude of the seasonal cycles. To check whether this occurred, we compared the length of the intervals using the DO3, DO4, and DO5.1 tie points. For the entire interval from DO3 to DO 5.1, WD2014 has a very similar number of years to GICC05, 27 (1%) fewer. The duration in the Hulu record is also quite similar with WD2014 finding 22 (1%) more years. This is a strong indication that the WD2014 is not consistently biased and years are not being skipped. However, the difference between WD2014 and GICC05 was much greater for the two shorter intervals between DO3 to DO4 and DO4 to DO5.1: WD2014 finds 146 (13%) more years than GICC05 in the interval between DO3 and DO4. Between DO4 and DO5.1, WD2014 finds 173 (9%) fewer years than GICC05. These differences are large enough that they are unlikely to be fully explained by Δ age and matching uncertainties and likely originate, at

CPD

11, 3425–3474, 2015

The WAIS Divide deep ice core WD2014 chronology

M. Sigl et al.

Title Page

Abstract

Introduction

Conclusions

References

Tables

Figures



Back

Close

Full Screen / Esc

Printer-friendly Version

Interactive Discussion



least partially, in the underlying annual layer interpretations. It is not currently possible to diagnose these differences in detail. We note that the WD2014 durations differ by 4 and 1 % from the Hulu durations for these shorter intervals.

4 Conclusions

WD2014 is the first multi-parameter, annual-layer based timescale extending into the last glacial for an Antarctic ice core. This was possible due to (1) the high annual snow-fall rates present at the drill site, (2) the small amount of layer thinning due to the thick ice and basal melting and (3) use of the most recent analytical techniques. The data included for the first time measurements of black carbon, a unique biomass-burning tracer with strong intra-annual emission variability arising from an insolation-driven annual biomass burning cycle in the Southern Hemisphere. Annual layers were continuously identified through the brittle ice zone using chemistry, which has not been done before, and with DEP. This allowed a continuous timescale to be developed without needing to match sections of multiple ice cores.

The age accuracy, as deduced by comparisons with absolutely dated timescales, is much better than the interpretation repeatability. The age accuracy for the Holocene (11 ka and younger) is estimated to be better than 0.5 % of the age; the age accuracy is estimated to increase to 1 % for ages older than 14.5 kaBP. WD2014 can become a reference chronology for Antarctic ice core records and the Southern Hemisphere equivalent of the Greenland GICC05 chronology. Synchronization between ice cores can be achieved using the WAIS Divide sulfur record of volcanic events, which does not require using the gas timescale and Δ age calculations, as demonstrated for the past 2000 years where 25 ice core records from Antarctica were synchronized to WAIS Divide (Sigl et al., 2014). Sulfate records are available for other deep ice-core records from East Antarctica including Vostok (Parrenin et al., 2012), Talos Dome (Severi et al., 2012), the EPICA cores from Dronning Maud Land, and Dome Concordia (Severi et al., 2007).

The WAIS Divide deep ice core WD2014 chronology

M. Sigl et al.

Title Page

Abstract

Introduction

Conclusions

References

Tables

Figures



Back

Close

Full Screen / Esc

Printer-friendly Version

Interactive Discussion



The WAIS Divide deep ice core WD2014 chronology

M. Sigl et al.

Title Page

Abstract

Introduction

Conclusions

References

Tables

Figures



Back

Close

Full Screen / Esc

Printer-friendly Version

Interactive Discussion



Banta, J. R., McConnell, J. R., Frey, M. M., Bales, R. C., and Taylor, K.: Spatial and temporal variability in snow accumulation at the West Antarctic Ice Sheet Divide over recent centuries, *J. Geophys. Res.-Atmos.*, 112, D10114, doi:10.1029/2006JD007887, 2008.

Baumgartner, M., Kindler, P., Eicher, O., Floch, G., Schilt, A., Schwander, J., Spahni, R., Capron, E., Chappellaz, J., Leuenberger, M., Fischer, H., and Stocker, T. F.: NGRIP CH₄ concentration from 120 to 10 kyr before present and its relation to a $\delta^{15}\text{N}$ temperature reconstruction from the same ice core, *Clim. Past*, 10, 903–920, doi:10.5194/cp-10-903-2014, 2014.

Bisiaux, M. M., Edwards, R., McConnell, J. R., Curran, M. A. J., Van Ommen, T. D., Smith, A. M., Neumann, T. A., Pasteris, D. R., Penner, J. E., and Taylor, K.: Changes in black carbon deposition to Antarctica from two high-resolution ice core records, 1850–2000 AD, *Atmos. Chem. Phys.*, 12, 4107–4115, doi:10.5194/acp-12-4107-2012, 2012.

Blockley, S. P. E., Lane, C. S., Hardiman, M., Rasmussen, S. O., Seierstad, I. K., Stefensen, J. P., Svensson, A., Lotter, A. F., Turney, C. S. M., and Bronk Ramsey, C.: Synchronisation of palaeoenvironmental records over the last 60,000 years, and an extended INTIMATE event stratigraphy to 48,000 b2k, *Quaternary Sci. Rev.*, 36, 2–10, 2012.

Blunier, T. and Brook, E. J.: Timing of millennial-scale climate change in Antarctica and Greenland during the last glacial period, *Science*, 291, 109–112, 2001.

Blunier, T., Spahni, R., Barnola, J.-M., Chappellaz, J., Loulergue, L., and Schwander, J.: Synchronization of ice core records via atmospheric gases, *Clim. Past*, 3, 325–330, doi:10.5194/cp-3-325-2007, 2007.

Bowman, D. M. J. S., Balch, J. K., Artaxo, P., Bond, W. J., Carlson, J. M., Cochrane, M. A., D'Antonio, C. M., DeFries, R. S., Doyle, J. C., Harrison, S. P., Johnston, F. H., Keeley, J. E., Krawchuk, M. A., Kull, C. A., Marston, J. B., Moritz, M. A., Prentice, I. C., Roos, C. I., Scott, A. C., Swetnam, T. W., van der Werf, G. R., and Pyne, S. J.: Fire in the earth system, *Science*, 324, 481–484, 2009.

Buizert, C., Cuffey, K. M., Severinghaus, J. P., Baggenstos, D., Fudge, T. J., Steig, E. J., Markle, B. R., Winstrup, M., Rhodes, R. H., Brook, E. J., Sowers, T. A., Clow, G. D., Cheng, H., Edwards, R. L., Sigl, M., McConnell, J. R., and Taylor, K. C.: The WAIS Divide deep ice core WD2014 chronology – Part 1: Methane synchronization (68–31 ka BP) and the gas age–ice age difference, *Clim. Past*, 11, 153–173, doi:10.5194/cp-11-153-2015, 2015.

The WAIS Divide deep ice core WD2014 chronology

M. Sigl et al.

[Title Page](#)

[Abstract](#)

[Introduction](#)

[Conclusions](#)

[References](#)

[Tables](#)

[Figures](#)



[Back](#)

[Close](#)

[Full Screen / Esc](#)

[Printer-friendly Version](#)

[Interactive Discussion](#)



Cole-Dai, J., Ferris, D., Lanciki, A., Savarino, J., Baroni, M., and Thiemens, M. H.: Cold decade (AD 1810–1819) caused by Tambora (1815) and another (1809) stratospheric volcanic eruption, *Geophys. Res. Lett.*, 36, L22703, doi:10.1029/2009gl040882, 2009.

Cole-Dai, J., Ferris, D. G., Lanciki, A. L., Savarino, J., Thiemens, M. H., and McConnell, J. R.: Two likely stratospheric volcanic eruptions in the 1450s CE found in a bipolar, subannually dated 800 year ice core record, *J. Geophys. Res.-Atmos.*, 118, 7459–7466, 2013.

Cole-Dai, J. H., Budner, D. M., and Ferris, D. G.: High speed, high resolution, and continuous chemical analysis of ice cores using a melter and ion chromatography, *Environ. Sci. Technol.*, 40, 6764–6769, 2006.

Cole-Dai, J. H., Mosley-Thompson, E., Wight, S. P., and Thompson, L. G.: A 4100 year record of explosive volcanism from an East Antarctica ice core, *J. Geophys. Res.-Atmos.*, 105, 24431–24441, 2000.

Edwards, R. L., Cheng, H., Wang, Y. J., Yuan, D. X., Kelly, M. J., Severinghaus, J. P., Burnett, A., Wang, X. F., Smith, E., and Kong, X. G.: A refined hulu and dongge cave climate record and the timing of climate change during the last glacial cycle, *Earth Planet. Sc. Lett.*, in review, 2015.

Ferretti, D. F., Miller, J. B., White, J. W. C., Etheridge, D. M., Lassey, K. R., Lowe, D. C., Meure, C. M. M., Dreier, M. F., Trudinger, C. M., van Ommen, T. D., and Langenfelds, R. L.: Unexpected changes to the global methane budget over the past 2000 years, *Science*, 309, 1714–1717, 2005.

Ferris, D. G., Cole-Dai, J., Reyes, A. R., and Budner, D. M.: South Pole ice core record of explosive volcanic eruptions in the first and second millennia AD and evidence of a large eruption in the tropics around 535 AD, *J. Geophys. Res.-Atmos.*, 116, D17308, doi:10.1029/2011JD015916, 2011.

Finkel, R. C. and Nishiizumi, K.: Beryllium 10 concentrations in the Greenland ice sheet project 2 ice core from 3–40 ka, *J. Geophys. Res.-Oceans.*, 102, 26699–26706, 1997.

Fischer, H., Fundel, F., Ruth, U., Twarloh, B., Wegner, A., Udisti, R., Becagli, S., Castellano, E., Morganti, A., Severi, M., Wolff, E., Littot, G., Rothlisberger, R., Mulvaney, R., Hutterli, M. A., Kaufmann, P., Federer, U., Lambert, F., Bigler, M., Hansson, M., Jonsell, U., de Angelis, M., Boutron, C., Siggaard-Andersen, M. L., Steffensen, J. P., Barbante, C., Gaspari, V., Gabrielli, P., and Wagenbach, D.: Reconstruction of millennial changes in dust emission, transport and regional sea ice coverage using the deep EPICA ice cores from the Atlantic and Indian Ocean sector of Antarctica, *Earth Planet. Sc. Lett.*, 260, 340–354, 2007.

The WAIS Divide deep ice core WD2014 chronology

M. Sigl et al.

Title Page

Abstract

Introduction

Conclusions

References

Tables

Figures



Back

Close

Full Screen / Esc

Printer-friendly Version

Interactive Discussion



Friedrich, M., Remmelel, S., Kromer, B., Hofmann, J., Spurk, M., Kaiser, K. F., Orcel, C., and Koppers, M.: The 12460 year Hohenheim oak and pine tree-ring chronology from central Europe – a unique annual record for radiocarbon calibration and paleoenvironment reconstructions, *Radiocarbon*, 46, 1111–1122, 2004.

5 Hammer, C. U.: Acidity of polar ice cores in relation to absolute dating, past volcanism, and radio-echoes, *J. Glaciol.*, 25, 359–372, 1980.

Hammer, C. U., Clausen, H. B., and Langway, C. C.: 50,000 years of recorded global volcanism, *Climatic Change*, 35, 1–15, 1997.

10 Hogg, A., Turney, C., Palmer, J., Southon, J., Kromer, B., Ramsey, C. B., Boswijk, G., Fenwick, P., Noronha, A., Staff, R., Friedrich, M., Reynard, L., Guetter, D., Wacker, L., and Jones, R.: The New Zealand Kauri (*Agathis Australis*) research project: a radiocarbon dating intercomparison of younger dryas wood and implications for intcal13, *Radiocarbon*, 55, 2035–2048, 2013.

15 Huber, C., Leuenberger, M., Spahni, R., Fluckiger, J., Schwander, J., Stocker, T. F., Johnsen, S., Landals, A., and Jouzel, J.: Isotope calibrated Greenland temperature record over marine isotope stage 3 and its relation to CH₄, *Earth Planet. Sc. Lett.*, 243, 504–519, doi:10.1016/j.epsl.2006.01.002, 2006.

Jacobel, R. W. and Welch, B. C.: A time marker at 17.5 kyr BP detected throughout West Antarctica, *Ann. Glaciol.*, 41, 47–51, 2005.

20 Jiang, S., Cole-Dai, J., Li, Y. S., Ferris, D. G., Ma, H. M., An, C. L., Shi, G. T., and Sun, B.: A detailed 2840 year record of explosive volcanism in a shallow ice core from dome A, East Antarctica, *J. Glaciol.*, 58, 65–75, 2012.

Lambert, F., Delmonte, B., Petit, J. R., Bigler, M., Kaufmann, P. R., Hutterli, M. A., Stocker, T. F., Ruth, U., Steffensen, J. P., and Maggi, V.: Dust-climate couplings over the past 800,000 years from the EPICA dome C ice core, *Nature*, 452, 616–619, 2008.

25 Lohne, O. S., Mangerud, J., and Birks, H. H.: Precise C-14 ages of the Vedde and Saksunarvatn ashes and the younger dryas boundaries from western Norway and their comparison with the Greenland ice core (GICC05) chronology, *J. Quaternary Sci.*, 28, 490–500, 2013.

30 Lohne, O. S., Mangerud, J., and Birks, H. H.: IntCal13 calibrated ages of the Vedde and Saksunarvatn ashes and the younger dryas boundaries from Krakenes, western Norway, *J. Quaternary Sci.*, 29, 506–507, 2014.

Lowe, J. J., Rasmussen, S. O., Bjorck, S., Hoek, W. Z., Steffensen, J. P., Walker, M. J. C., Yu, Z. C., and Grp, I.: Synchronisation of palaeoenvironmental events in the North Atlantic

The WAIS Divide deep ice core WD2014 chronology

M. Sigl et al.

[Title Page](#)

[Abstract](#)

[Introduction](#)

[Conclusions](#)

[References](#)

[Tables](#)

[Figures](#)



[Back](#)

[Close](#)

[Full Screen / Esc](#)

[Printer-friendly Version](#)

[Interactive Discussion](#)



region during the Last Termination: a revised protocol recommended by the INTIMATE group, *Quaternary Sci. Rev.*, 27, 6–17, 2008.

Marcott, S. A., Bauska, T. K., Buizert, C., Steig, E. J., Rosen, J. L., Cuffey, K. M., Fudge, T. J., Severinghaus, J. P., Ahn, J., Kalk, M. L., McConnell, J. R., Sowers, T., Taylor, K. C., White, J. W. C., and Brook, E. J.: Centennial-scale changes in the global carbon cycle during the last deglaciation, *Nature*, 514, 616–619, 2014.

McConnell, J. R.: Continuous ice-core chemical analyses using inductively Coupled Plasma Mass Spectrometry, *Environ. Sci. Technol.*, 36, 7–11, 2002.

McConnell, J. R.: New Directions: historical black carbon and other ice core aerosol records in the Arctic for GCM evaluation, *Atmos. Environ.*, 44, 2665–2666, 2010.

McConnell, J. R. and Edwards, R.: Coal burning leaves toxic heavy metal legacy in the Arctic, *P. Natl. Acad. Sci. USA*, 105, 12140–12144, 2008.

McConnell, J. R., Aristarain, A. J., Banta, J. R., Edwards, P. R., and Simoes, J. C.: 20th-Century doubling in dust archived in an Antarctic Peninsula ice core parallels climate change and desertification in South America, *P. Natl. Acad. Sci. USA*, 104, 5743–5748, 2007.

McConnell, J. R., Maselli, O. J., Sigl, M., Vallelonga, P., Neumann, T., Anschutz, H., Bales, R. C., Curran, M. A. J., Das, S. B., Edwards, R., Kipfstuhl, S., Layman, L., and Thomas, E. R.: Antarctic-wide array of high-resolution ice core records reveals pervasive lead pollution began in 1889 and persists today, *Sci. Rep.-UK*, 4, 5848, doi:10.1038/srep05848, 2014.

McGwire, K. C., Taylor, K. C., Banta, J. R., and McConnell, J. R.: Identifying annual peaks in dielectric profiles with a selection curve, *J. Glaciol.*, 57, 763–769, 2011.

Miyake, F., Nagaya, K., Masuda, K., and Nakamura, T.: A signature of cosmic-ray increase in AD 774–775 from tree rings in Japan, *Nature*, 486, 240–242, 2012.

Monnin, E., Indermuhle, A., Dallenbach, A., Fluckiger, J., Stauffer, B., Stocker, T. F., Raynaud, D., and Barnola, J. M.: Atmospheric CO₂ concentrations over the last glacial termination, *Science*, 291, 112–114, 2001.

Moore, John, C. et al. The chemical basis for the electrical stratigraphy of ice, *J. Geophys. Res.-Sol. Ea.*, 97, 1887–1896, 1992.

Muscheler, R., Adolphi, F., and Knudsen, M. F.: Assessing the differences between the IntCal and Greenland ice-core time scales for the last 14,000 years via the common cosmogenic radionuclide variations, *Quaternary Sci. Rev.*, 106, 81–87, 2014.

The WAIS Divide deep ice core WD2014 chronology

M. Sigl et al.

[Title Page](#)

[Abstract](#)

[Introduction](#)

[Conclusions](#)

[References](#)

[Tables](#)

[Figures](#)



[Back](#)

[Close](#)

[Full Screen / Esc](#)

[Printer-friendly Version](#)

[Interactive Discussion](#)



Muscheler, R., Kromer, B., Björck, S., Svensson, A., Friedrich, M., Kaiser, K. F., and Southon, J.: Tree rings and ice cores reveal C-14 calibration uncertainties during the younger dryas, *Nat. Geosci.*, 1, 263–267, 2008.

NGRIP-Project-Members: High-resolution record of Northern Hemisphere climate extending into the last interglacial period, *Nature*, 431, 147–151, 2004.

Nishiizumi, K., Imamura, M., Caffee, M. W., Southon, J. R., Finkel, R. C., and McAninch, J.: Absolute calibration of Be-10 AMS standards, *Nucl. Instrum. Meth. B*, 258, 403–413, 2007.

Oeschger, H., Siegenthaler, U., Schotterer, U., and Gugelmann, A.: Box diffusion-model to study carbon-dioxide exchange in nature, *Tellus*, 27, 168–192, 1975.

Parrenin, F., Petit, J.-R., Masson-Delmotte, V., Wolff, E., Basile-Doelsch, I., Jouzel, J., Lipenkov, V., Rasmussen, S. O., Schwander, J., Severi, M., Udisti, R., Veres, D., and Vinther, B. M.: Volcanic synchronisation between the EPICA Dome C and Vostok ice cores (Antarctica) 0–145 kyr BP, *Clim. Past*, 8, 1031–1045, doi:10.5194/cp-8-1031-2012, 2012.

Pasteris, D., McConnell, J. R., Edwards, R., Isaksson, E., and Albert, M. R.: Acidity decline in Antarctic ice cores during the Little Ice Age linked to changes in atmospheric nitrate and sea salt concentrations, *J. Geophys. Res.-Atmos.*, 119, 5640–5652, 2014a.

Pasteris, D. R., McConnell, J. R., Das, S. B., Criscitiello, A. S., Evans, M. J., Maselli, O. J., Sigl, M., and Layman, L.: Seasonally resolved ice core records from West Antarctica indicate a sea ice source of sea-salt aerosol and a biomass burning source of ammonium, *J. Geophys. Res.-Atmos.*, 119, 9168–9182, 2014b.

Pasteris, D. R., McConnell, J. R., and Edwards, R.: High-Resolution, Continuous Method for Measurement of Acidity in Ice Cores, *Environ. Sci. Technol.*, 46, 1659–1666, 2012.

Petherick, L., Bostock, H., Cohen, T. J., Fitzsimmons, K., Tibby, J., Fletcher, M. S., Moss, P., Reeves, J., Mooney, S., Barrows, T., Kemp, J., Jansen, J., Nanson, G., and Dosseto, A.: Climatic records over the past 30 ka from temperate Australia – a synthesis from the OZINTIMATE workgroup, *Quaternary Sci. Rev.*, 74, 58–77, 2013.

Raisbeck, G. M., Yiou, F., Jouzel, J., and Stocker, T. F.: Direct north-south synchronization of abrupt climate change record in ice cores using Beryllium 10, *Clim. Past*, 3, 541–547, doi:10.5194/cp-3-541-2007, 2007.

Rasmussen, S. O., Andersen, K. K., Svensson, A. M., Steffensen, J. P., Vinther, B. M., Clausen, H. B., Siggaard-Andersen, M. L., Johnsen, S. J., Larsen, L. B., Dahl-Jensen, D., Bigler, M., Rothlisberger, R., Fischer, H., Goto-Azuma, K., Hansson, M. E., and Ruth, U.:

The WAIS Divide deep ice core WD2014 chronology

M. Sigl et al.

[Title Page](#)[Abstract](#)[Introduction](#)[Conclusions](#)[References](#)[Tables](#)[Figures](#)[Back](#)[Close](#)[Full Screen / Esc](#)[Printer-friendly Version](#)[Interactive Discussion](#)

A new Greenland ice core chronology for the last glacial termination, *J. Geophys. Res.-Atmos.*, 111, 2006.

Rasmussen, S. O., Bigler, M., Blockley, S. P., Blunier, T., Buchardt, S. L., Clausen, H. B., Cvi-
janovic, I., Dahl-Jensen, D., Johnsen, S. J., Fischer, H., Gkinis, V., Guillevic, M., Hoek, W. Z.,
5 Lowe, J. J., Pedro, J. B., Popp, T., Seierstad, I. K., Steffensen, J. P., Svensson, A. M., Valle-
longa, P., Vinther, B. M., Walker, M. J. C., Wheatley, J. J., and Winstrup, M.: A stratigraphic
framework for abrupt climatic changes during the Last Glacial period based on three synchron-
ized Greenland ice-core records: refining and extending the INTIMATE event stratigraphy,
Quaternary Sci. Rev., 106, 14–28, 2014.

10 Reimer, P. J., Bard, E., Bayliss, A., Beck, J. W., Blackwell, P. G., Ramsey, C. B., Buck, C. E.,
Cheng, H., Edwards, R. L., Friedrich, M., Grootes, P. M., Guilderson, T. P., Hafliadason, H.,
Hajdas, I., Hatte, C., Heaton, T. J., Hoffmann, D. L., Hogg, A. G., Hughen, K. A., Kaiser, K. F.,
Kromer, B., Manning, S. W., Niu, M., Reimer, R. W., Richards, D. A., Scott, E. M.,
Southon, J. R., Staff, R. A., Turney, C. S. M., and van der Plicht, J.: Intcal13 and Marine13 ra-
15 diocarbon age calibration curves 0–50,000 years cal Bp, *Radiocarbon*, 55, 1869–1887, 2013.

Rosen, J. L., Brook, E. J., Severinghaus, J. P., Blunier, T., Mitchell, L. E., Lee, J. E., Ed-
wards, J. S., and Gkinis, V.: An ice core record of near-synchronous global climate changes
at the Bolling transition, *Nat. Geosci.*, 7, 459–463, 2014.

Ruth, U., Wagenbach, D., Steffensen, J. P., and Bigler, M.: Continuous record of microparticle
concentration and size distribution in the central Greenland NGRIP ice core during the last
20 glacial period, *J. Geophys. Res.-Atmos.*, 108, 2003.

Schultz, M. G., Heil, A., Hoelzemann, J. J., Spessa, A., Thonicke, K., Goldammer, J. G.,
Held, A. C., Pereira, J. M. C., and van het Bolscher, M.: Global wildland fire emissions from
1960 to 2000, *Global Biogeochem. Cy.*, 22, 2008.

25 Schwarz, J. P., Gao, R. S., Fahey, D. W., Thomson, D. S., Watts, L. A., Wilson, J. C.,
Reeves, J. M., Darbeheshti, M., Baumgardner, D. G., Kok, G. L., Chung, S. H., Schulz, M.,
Hendricks, J., Lauer, A., Karcher, B., Slowik, J. G., Rosenlof, K. H., Thompson, T. L., Lang-
ford, A. O., Loewenstein, M., and Aikin, K. C.: Single-particle measurements of midlatitude
black carbon and light-scattering aerosols from the boundary layer to the lower stratosphere,
J. Geophys. Res.-Atmos., 111, 2006.

30 Severi, M., Becagli, S., Castellano, E., Morganti, A., Traversi, R., Udisti, R., Ruth, U., Fischer, H.,
Huybrechts, P., Wolff, E., Parrenin, F., Kaufmann, P., Lambert, F., and Steffensen, J. P.: Syn-

**The WAIS Divide
deep ice core
WD2014 chronology**

M. Sigl et al.

[Title Page](#)[Abstract](#)[Introduction](#)[Conclusions](#)[References](#)[Tables](#)[Figures](#)[Back](#)[Close](#)[Full Screen / Esc](#)[Printer-friendly Version](#)[Interactive Discussion](#)

chronisation of the EDML and EDC ice cores for the last 52 kyr by volcanic signature matching, *Clim. Past*, 3, 367–374, doi:10.5194/cp-3-367-2007, 2007.

Severi, M., Udisti, R., Becagli, S., Stenni, B., and Traversi, R.: Volcanic synchronisation of the EPICA-DC and TALDICE ice cores for the last 42 kyr BP, *Clim. Past*, 8, 509–517, doi:10.5194/cp-8-509-2012, 2012.

Siegenthaler, U.: Uptake of Excess CO₂ by an Outcrop-Diffusion Model of the Ocean, *J. Geophys. Res.-Oc. Atm.*, 88, 3599–3608, 1983.

Siegenthaler, U., Stocker, T. F., Monnin, E., Luthi, D., Schwander, J., Stauffer, B., Raynaud, D., Barnola, J. M., Fischer, H., Masson-Delmotte, V., and Jouzel, J.: Stable carbon cycle–climate relationship during the late Pleistocene, *Science*, 310, 1313–1317, 2005.

Sigl, M., McConnell, J. R., Layman, L., Maselli, O., McGwire, K., Pasteris, D., Dahl-Jensen, D., Steffensen, J. P., Vinther, B., Edwards, R., Mulvaney, R., and Kipfstuhl, S.: A new bipolar ice core record of volcanism from WAIS Divide and NEEM and implications for climate forcing of the last 2000 years, *J. Geophys. Res.-Atmos.*, 118, 1151–1169, 2013.

Sigl, M., McConnell, J. R., Toohey, M., Curran, M., Das, S. B., Edwards, R., Isaksson, E., Kawamura, K., Kipfstuhl, S., Krüger, K., Layman, L., Maselli, O. J., Motizuki, Y., Motoyama, H., Pasteris, D. R., and Severi, M.: Insights from Antarctica on volcanic forcing during the Common Era, *Nature Climate Change*, 4, 693–697, 2014.

Sigl, M., Winstrup, M., McConnell, J. R., Welten, K. C., Plunkett, G., Ludlow, F., Büntgen, U., Caffee, M. W., Chellman, N. J., Dahl-Jensen, D., Fischer, H., Kipfstuhl, S., Kostick, C., Maselli, O. J., Mekhaldi, F., Mulvaney, R., Muscheler, R., Pasteris, D. R., Pilcher, J. R., Salzer, M., Schüpbach, S., Steffensen, J. P., Vinther, B., and Woodruff, T. E.: Timing and climate forcing of volcanic eruptions for the past 2500 years, *Nature*, doi:10.1038/nature14565, 2015.

Souney, J. M., Twickler, M. S., Hargreaves, G., Benciveno, B. M., Kippenhan, M., Johnson, J. A., Cravens, E. D., Neff, P. D., Nunn, R. M., Orsi, A. J., Popp, T., Rhoades, J. F., Vaughn, B. H., Voigt, D. E., Wong, G. J., and Taylor, K. C.: Core handling and processing for the WAIS Divide ice-core project, *J. Glaciol.*, 55, 15–26, 2014.

Steinhilber, F., Abreu, J. A., Beer, J., Brunner, I., Christl, M., Fischer, H., Heikkilä, U., Kubik, P. W., Mann, M., McCracken, K. G., Miller, H., Miyahara, H., Oerter, H., and Wilhelms, F.: 9400 years of cosmic radiation and solar activity from ice cores and tree rings, *P. Natl. Acad. Sci. USA*, 109, 5967–5971, 2012.

The WAIS Divide deep ice core WD2014 chronology

M. Sigl et al.

Title Page

Abstract

Introduction

Conclusions

References

Tables

Figures



Back

Close

Full Screen / Esc

Printer-friendly Version

Interactive Discussion



- Svensson, A., Andersen, K. K., Bigler, M., Clausen, H. B., Dahl-Jensen, D., Davies, S. M., Johnsen, S. J., Muscheler, R., Rasmussen, S. O., Rothlisberger, R., Steffensen, J. P., and Vinther, B. M.: The Greenland ice core chronology 2005, 15–42 ka, Part 2: Comparison to other records, *Quaternary Sci. Rev.*, 25, 3258–3267, 2006.
- 5 Svensson, A., Andersen, K. K., Bigler, M., Clausen, H. B., Dahl-Jensen, D., Davies, S. M., Johnsen, S. J., Muscheler, R., Parrenin, F., Rasmussen, S. O., Röthlisberger, R., Seierstad, I., Steffensen, J. P., and Vinther, B. M.: A 60 000 year Greenland stratigraphic ice core chronology, *Clim. Past*, 4, 47–57, doi:10.5194/cp-4-47-2008, 2008.
- Taylor, K. C., Alley, R. B., Lamorey, G. W., and Mayewski, P.: Electrical measurements on the
10 Greenland Ice Sheet Project 2 core, *J. Geophys. Res.-Oceans.*, 102, 26511–26517, 1997.
- van der Werf, G. R., Randerson, J. T., Giglio, L., Collatz, G. J., Mu, M., Kasibhatla, P. S., Morton, D. C., DeFries, R. S., Jin, Y., and van Leeuwen, T. T.: Global fire emissions and the contribution of deforestation, savanna, forest, agricultural, and peat fires (1997–2009), *Atmos. Chem. Phys.*, 10, 11707–11735, doi:10.5194/acp-10-11707-2010, 2010.
- 15 Vonmoos, M., Beer, J., and Muscheler, R.: Large variations in Holocene solar activity: constraints from Be-10 in the Greenland Ice Core Project ice core, *J. Geophys. Res.-Space*, 111, A10105, doi:10.1029/2005JA011500, 2006.
- WAIS Divide Project Members: Onset of deglacial warming in West Antarctica driven by local orbital forcing, *Nature*, 500, 440–444, 2013.
- 20 Wang, Y. J., Cheng, H., Edwards, R. L., An, Z. S., Wu, J. Y., Shen, C. C., and Dorale, J. A.: A high-resolution absolute-dated late Pleistocene monsoon record from Hulu Cave, China, *Science*, 294, 2345–2348, 2001.
- Wang, Y. J., Cheng, H., Edwards, R. L., He, Y. Q., Kong, X. G., An, Z. S., Wu, J. Y., Kelly, M. J., Dykoski, C. A., and Li, X. D.: The Holocene Asian monsoon: links to solar changes and North Atlantic climate, *Science*, 308, 854–857, 2005.
- 25 Weber, M. E., Clark, P. U., Kuhn, G., Timmermann, A., Spreng, D., Gladstone, R., Zhang, X., Lohmann, G., Menviel, L., Chikamoto, M. O., Friedrich, T., and Ohlwein, C.: Millennial-scale variability in Antarctic ice-sheet discharge during the last deglaciation, *Nature*, 510, 134–138, 2014.
- 30 Winstrup, M., Svensson, A. M., Rasmussen, S. O., Winther, O., Steig, E. J., and Axelrod, A. E.: An automated approach for annual layer counting in ice cores, *Clim. Past*, 8, 1881–1895, doi:10.5194/cp-8-1881-2012, 2012.

The WAIS Divide deep ice core WD2014 chronology

M. Sigl et al.

Table 2. Constructing the WD2014 ice core chronology: annual-layer interpretation results using various data and interpretation techniques.

Depth interval (m)	–577	577–1300	1300–1940	1940–2020 ^a	2020–2274	2274–2300	2300–2711	2711–2800	2800–2850		
Bottom age (Yr BP 1950)	2345	6009	11 362	12 146	14 980	15 302	26 872	29 460	31 247		
Mean annual layer thickness λ (cm)	24.	19.7	12.	10.2	9.	8.1	3.6	3.4	2.8		
Interpretation method											
Number annual layers (rel. to WD2014)											
Consensus decision											
I	ECM	Selection curve	N/A	3704 +40 (1.1 %)	5396 +43 (0.8 %)	N/A	2855 +21 (0.7 %)	322 (0.0 %)	11 567 –3 (0.0 %)	2585 –3 (–0.1 %)	N/A
II	Aerosols	Manual	2415 +13 (0.5 %)	3668 +4 (0.1 %)	5368 +15 (0.3 %)	N/A	2843 +9 (0.3 %)	321 –1 (–0.3 %)	N/A	N/A	N/A
III	Aerosols	StratiCounter	2402 ^b (0 %)	N/A	5310 –43 (–0.8 %)	768 –16 (–2.0 %)	2645 –189 (–6.7 %)	N/A	N/A	2649 ^c +61 (+2.4 %)	N/A

N/A ice core section was not annually dated with the respective dating method/data.

^a The depth interval from 1940 to 2020 m was originally interpreted by using the combined aerosol and ECM data sets (WAIS Divide Project Members, 2013).

^b The StratiCounter algorithm was run starting from 188 m depth (12:56 CE), with the uppermost part of the timescale being adopted as is.

^c This section is based only on particle concentration data from the aerosol data set.

[Title Page](#)
[Abstract](#)
[Introduction](#)
[Conclusions](#)
[References](#)
[Tables](#)
[Figures](#)

[Back](#)
[Close](#)
[Full Screen / Esc](#)
[Printer-friendly Version](#)
[Interactive Discussion](#)


The WAIS Divide deep ice core WD2014 chronology

M. Sigl et al.

Table 3. Comparison of the WD2014 ice core chronology to independent chronologies Hulu cave (Wang et al., 2011; Buizert et al., 2015; Edwards et al., 2015) and tree-ring based IntCal13 radiocarbon curve (Reimer et al., 2013). A detailed description and discussion for the WAIS Divide Δ age estimation and synchronization procedures between the WAIS Divide CH_4 record Hulu $\delta^{18}\text{O}_{\text{Calcite}}$ record is provided by Buizert et al. (2015).

Climate event or comparison point	Age in WD2014	Comparison record	Age in comparison record (yrBP 1950)	age difference (%) between records
8.5 ka (WAIS Divide offset older maximum)	8500	Intcal13	8516	16 years (0.2%)
10.5 ka (WD offset younger maximum)	10 500	Intcal13	10 490	10 years (0.1%)
Onset of DO3	27 755	Hulu	27 922 \pm 95	167 years (0.6%)
Onset of DO4	29 011	Hulu	29 134 \pm 92	123 years (0.4%)
Onset of DO5.1	30 730	Hulu	30 876 \pm 255	146 years (0.5%)

Title Page

Abstract

Introduction

Conclusions

References

Tables

Figures



Back

Close

Full Screen / Esc

Printer-friendly Version

Interactive Discussion



The WAIS Divide deep ice core WD2014 chronology

M. Sigl et al.

Table 4. Comparison to the independent chronologies from NGRIP (Andersen et al., 2006; Rasmussen et al., 2006; Svensson et al., 2006), and Kråkenes Lake (Lohne et al., 2013, 2014). A detailed description and discussion for the WAIS Divide Δ age estimation and synchronization procedures between the WAIS Divide CH_4 record and NGRIP $\delta^{18}\text{O}$ is provided by Buizert et al. (2015).

Climate transition	WAIS Divide (WD2014)			NGRIP (GICC05)		Kråkenes (Intcal13) Age interval (2σ)
	Depth (m)	Ice age (yrBP 1950)	Gas age (yrBP 1950)	Depth (m) (yrBP 1950)	Ice age $\pm 2\sigma$ (yrBP 1950)	
YD-PB	1983.02	11 740 \pm 74	11 546 \pm 78	1490.89	11 619 \pm 98	11 655–11 419
BA-YD	2096.61	12 987 \pm 106	12 769 \pm 111	1524.20	12 775 \pm 136	12 809–12 680
OD-BA	2259.40	14 804 \pm 148	14 576 \pm 151	1604.05	14 628 \pm 185	
DO 3 (termination)	2747.25	27 905 \pm 279	27 521 \pm 293	1861.90	27 498 \pm 822	
DO 3 (onset)	2755.74	28 144 \pm 281	27 755 \pm 295	1869.00	27 728 \pm 832	
DO 4 (termination)	2787.99	29 091 \pm 291	28 696 \pm 304	1882.60	28 548 \pm 887	
DO 4 (onset)	2797.92	29 396 \pm 294	29 011 \pm 306	1891.27	28 838 \pm 898	
DO 5.1 (termination)	2845.37	31 067 \pm 311	30 618 \pm 328	1916.50	30 571 \pm 1010	
DO 5.1 (onset)	2848.38	31 186 \pm 312	30 730 \pm 329	1919.48	30 731 \pm 1023	

Title Page

Abstract

Introduction

Conclusions

References

Tables

Figures



Back

Close

Full Screen / Esc

Printer-friendly Version

Interactive Discussion



The WAIS Divide deep ice core WD2014 chronology

M. Sigl et al.

Table 5. Comparison of interval durations between WD2014, GICC05 (NGRIP-Project-Members, 2004) and Hulu cave (Edwards et al., in review) chronologies. Years of difference are given as reference – WD2014. We use a Greenland-CH₄ phasing of 50 ± 30 years for the Younger Dryas (YD) to Preboreal (PB) transition, 45 ± 30 years for the Older Dryas (OD) to Bølling-Allerød (BA) transition and a phasing 25 ± 30 years for all other transitions (Rosen et al., 2014; Buizert et al., 2015). We assume no age difference between Hulu and CH₄ during the transition of DO 5.1, DO 4 and DO 3.

	WD2014	GICC05	Hulu
YD/PB to BA/YD	1199	1156 –43 (–4 %)	NA NA
BA/YD to OD/BA	1827	1853 26 (1 %)	NA
DO3 to DO4	1256	1110 –146 (–12 %)	1212 –44 (–4 %)
DO4 to DO5.1	1720	1893 173 (10 %)	1742 23 (1 %)
DO3 to DO5.1	2976	3003 27 (0.9 %)	2954 –21 (–0.7 %)

NA = not analyzed

[Title Page](#)[Abstract](#)[Introduction](#)[Conclusions](#)[References](#)[Tables](#)[Figures](#)[Back](#)[Close](#)[Full Screen / Esc](#)[Printer-friendly Version](#)[Interactive Discussion](#)

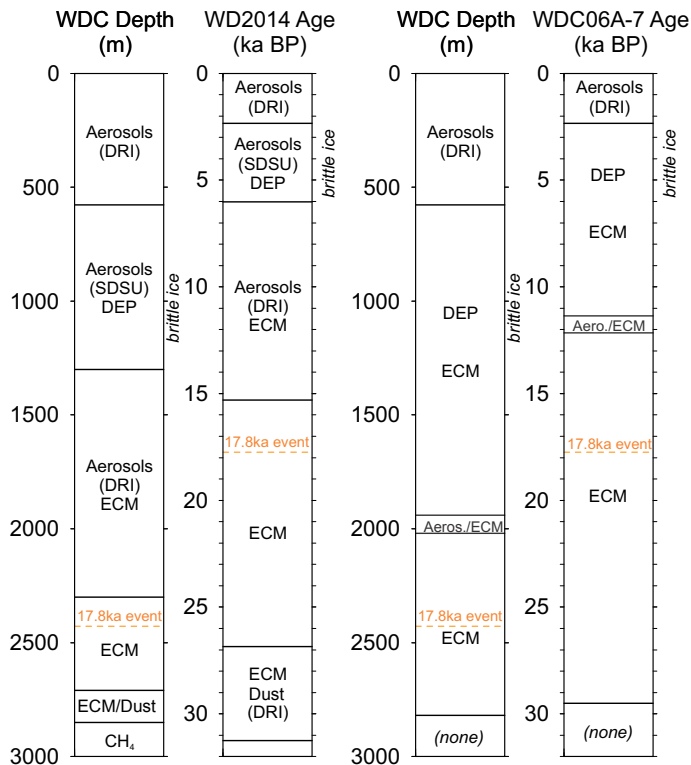


Figure 1. Overview of the data sets used for development of WAIS-Divide annual-layer dating chronologies. (Left): depth and age information for the WAIS Divide aerosol records obtained at the Desert Research Institute (DRI) and South Dakota State University (SDSU), and ECM/DEP data used to establish the new WD2014 chronology. (Right): data sets used for development of the previous WDC06A-7 chronology. Also shown is the position of the acidity anomaly (17.8 ka event), a major chrono-stratigraphic age marker across West Antarctica (Hammer et al., 1997; Jacobel and Welch, 2005). Aerosol data below 2300 m (> 15 kaBP) is from insoluble particle measurements (i.e., dust) only.

The WAIS Divide deep ice core WD2014 chronology

M. Sigl et al.

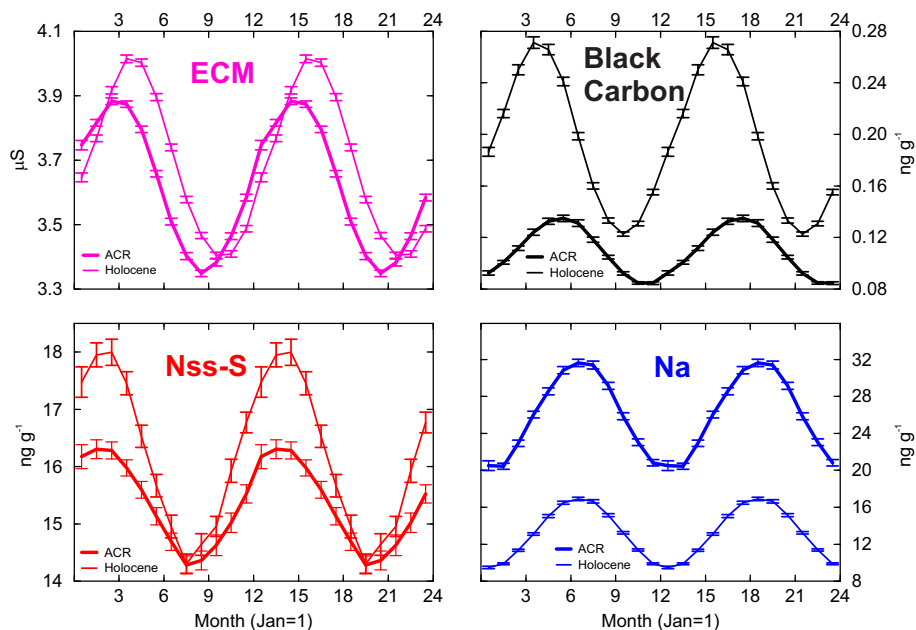


Figure 2. Average annual cycle computed for WAIS Divide ECM record and aerosol records of Na, nssS, and BC for a 1000 year period centered over the early Holocene (10–11 kaBP, thin line) and Antarctic Cold Reversal (ACR) (13–14 kaBP, bold line), respectively. Shown are average monthly values for two complete annual cycles (January = month 1) assuming constant snowfall distribution throughout the year. Uncertainty bars are 1σ standard error of the mean. Average WAIS Divide annual-layer thickness for the investigated time intervals is $10.0 \pm 1.6 \text{ cm a}^{-1}$ (Holocene) and $9.2 \pm 1.4 \text{ cm a}^{-1}$ (ACR), respectively.

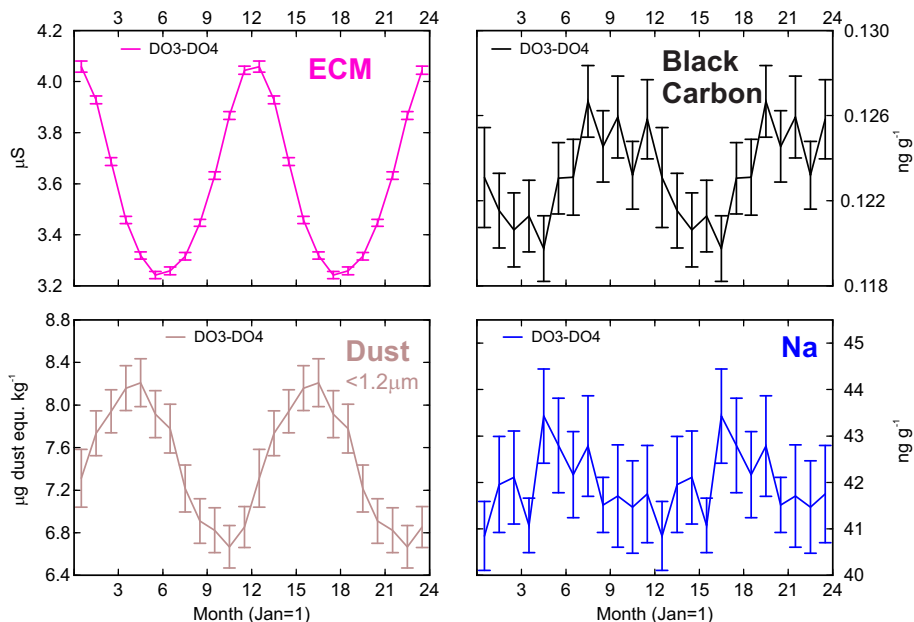


Figure 3. Average annual cycles for WAIS Divide aerosol records similar to Fig. 2, but for a 1250 year period between the onset of Dansgaard/Oeschger (DO) events 3 and 4 (i.e., 28.1–29.4 kaBP), as determined from the WAIS Divide CH₄ record (Buizert et al., 2015). Shown are average monthly values for two complete annual cycles (January = month 1) assuming constant snowfall distribution throughout the year. Uncertainty bars are 1 σ standard error of the mean. Average WAIS Divide annual layer thickness for this interval is $3.4 \pm 0.7 \text{ cm a}^{-1}$.

Title Page

Abstract

Introduction

Conclusions

References

Tables

Figures



Back

Close

Full Screen / Esc

Printer-friendly Version

Interactive Discussion



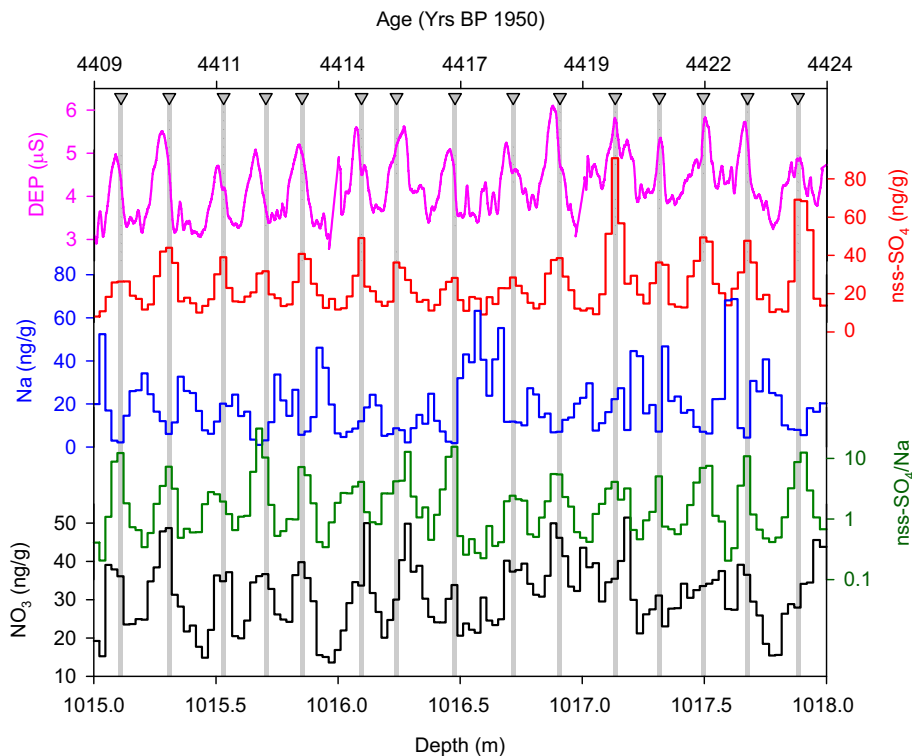


Figure 4. Example of a 3 m long ice core section within the WAIS Divide brittle ice zone (approximately 4400 years BP), a section for which ice core sample quality was rated poorest (Souney et al., 2014). WD2014 annual-layer markers (triangles with grey lines) are indicated. Annual layers are identified by summer and winter tracers: winters are characterized by maxima in $[\text{Na}^+]$, summers are characterized by maxima in $[\text{NO}_3^-]$, $[\text{nss-SO}_4^{2-}]$ and corresponding DEP maxima. Also shown is the ratio of $[\text{nss-SO}_4^{2-}]/[\text{Na}^+]$.

The WAIS Divide
deep ice core
WD2014 chronology

M. Sigl et al.

Title Page

Abstract

Introduction

Conclusions

References

Tables

Figures



Back

Close

Full Screen / Esc

Printer-friendly Version

Interactive Discussion



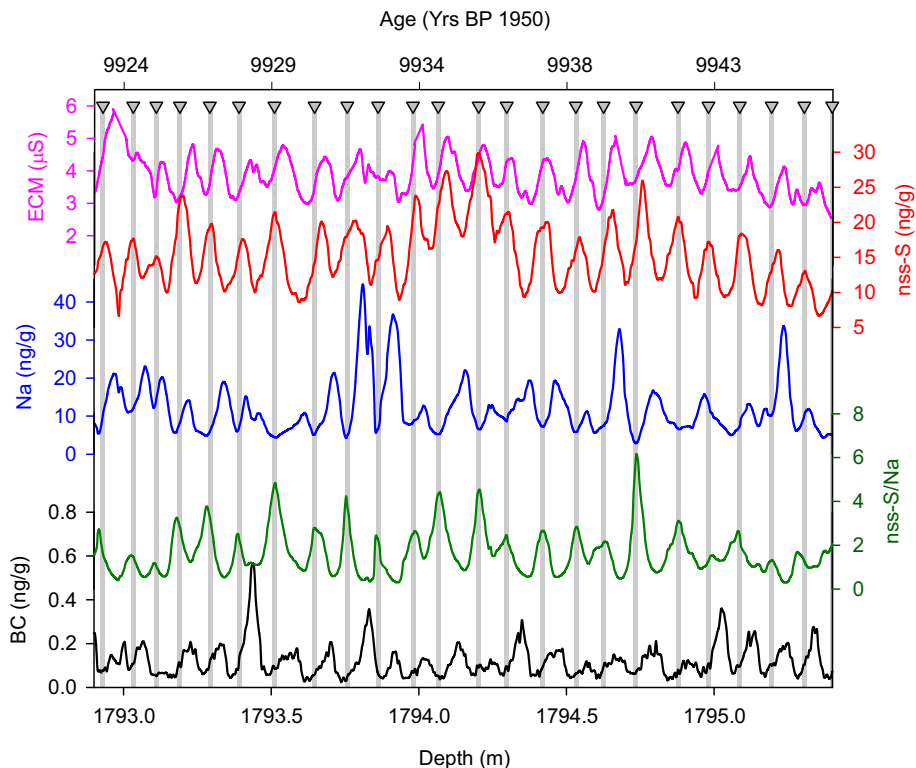


Figure 5. Example of a 2.5m long ice core section of WAIS Divide (approximately 9900 years BP) with annual-layer markers (triangles with grey lines) indicated. Annual layers are here identified by matching pairs of winter, spring, and summer tracers. Summers are characterized by maxima in [nss-S] and corresponding ECM maxima; autumn is indicated by maxima in [BC] from biomass burning, whereas the [Na] records show maxima in winter. Also shown is the ratio of [nss-S]/[Na].

The WAIS Divide
deep ice core
WD2014 chronology

M. Sigl et al.

Title Page

Abstract

Introduction

Conclusions

References

Tables

Figures



Back

Close

Full Screen / Esc

Printer-friendly Version

Interactive Discussion



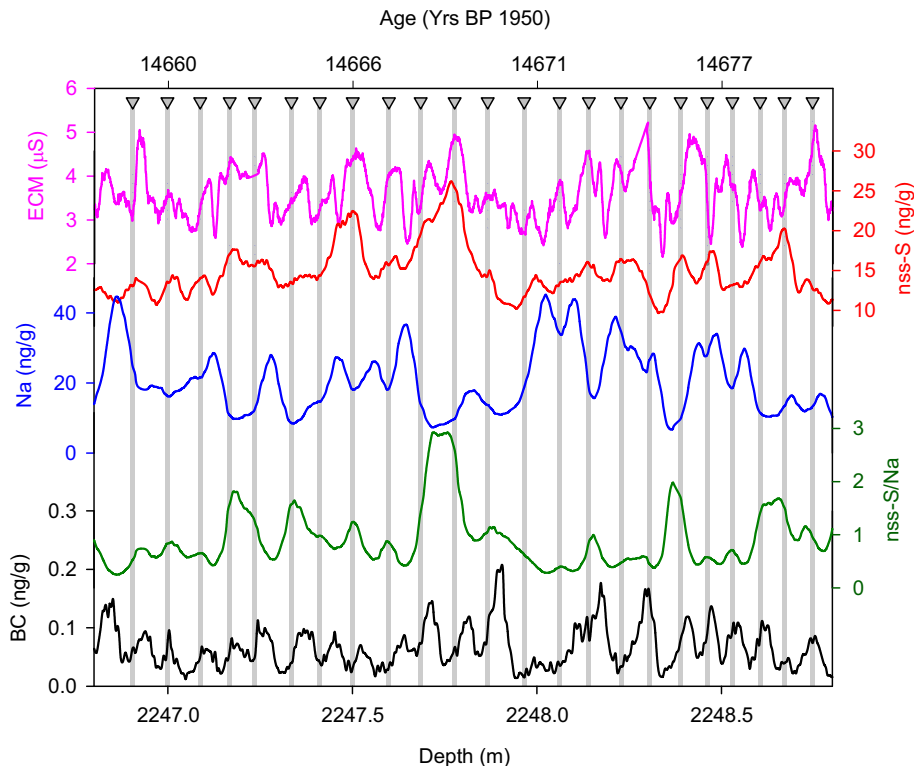


Figure 6. Example of a 2m long ice core section of WAIS Divide (approximately 14 700 years BP) with annual-layer markers (triangles with grey lines) indicated. Similar to Fig. 5, annual layers are identified by matching pairs of winter, spring, and summer tracers. [Na] and [nss-S], determined by ICPMS, do not always show clear annual cycles in this section with an average layer thickness of 8 cm a^{-1} thus limiting their use for annual-layer dating in the deeper part of WAIS Divide. Annual layers are identified here using the autumn maxima in [BC] and the summer maxima in the ECM record, respectively.

The WAIS Divide
deep ice core
WD2014 chronology

M. Sigl et al.

Title Page

Abstract

Introduction

Conclusions

References

Tables

Figures

◀

▶

◀

▶

Back

Close

Full Screen / Esc

Printer-friendly Version

Interactive Discussion



The WAIS Divide deep ice core WD2014 chronology

M. Sigl et al.

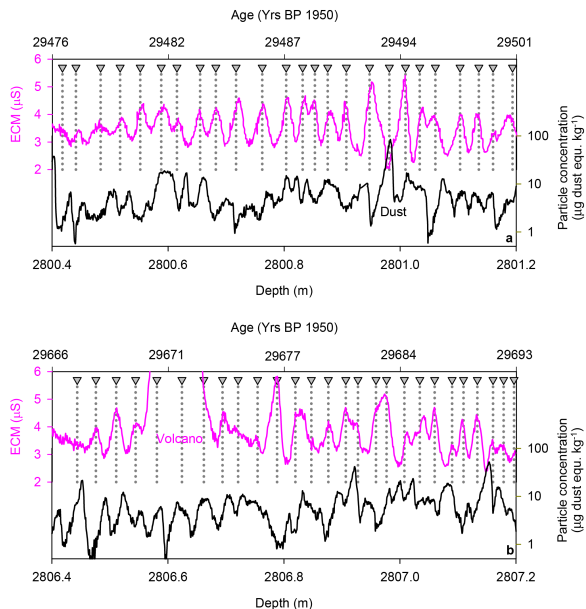


Figure 7. Example of two 0.8 m long ice core sections of WD from **(a)** approximately 29 500 and **(b)** 29 700 years BP 1950, respectively, with annual-layer markers indicated. Annual layers are here identified by matching pairs of winter and summer tracers. Summers are characterized by ECM maxima. Winters are indicated by maxima in dust deposition derived from the WD insoluble particle concentration record using the particle size range $< 1.2 \mu\text{m}$ typical for dust being transported over large distances. Dust concentrations are shown on a logarithmic scale. Also shown is an example (2801 m) of how dust input can mask annual cycles in the ECM record by neutralizing acids present in the snowpack that usually are responsible for the annual cycle observed in electrical properties in the ice **(a)**. The insoluble dust record provides confident and independent information on annual layering at WAIS Divide, also in the presence of acidity excursions caused by large volcanic eruptions as indicated by a four-year long period of increased acidity content centred at 2806.6 m depth **(b)**.

[Title Page](#)
[Abstract](#)
[Introduction](#)
[Conclusions](#)
[References](#)
[Tables](#)
[Figures](#)

[Back](#)
[Close](#)
[Full Screen / Esc](#)
[Printer-friendly Version](#)
[Interactive Discussion](#)


The WAIS Divide deep ice core WD2014 chronology

M. Sigl et al.

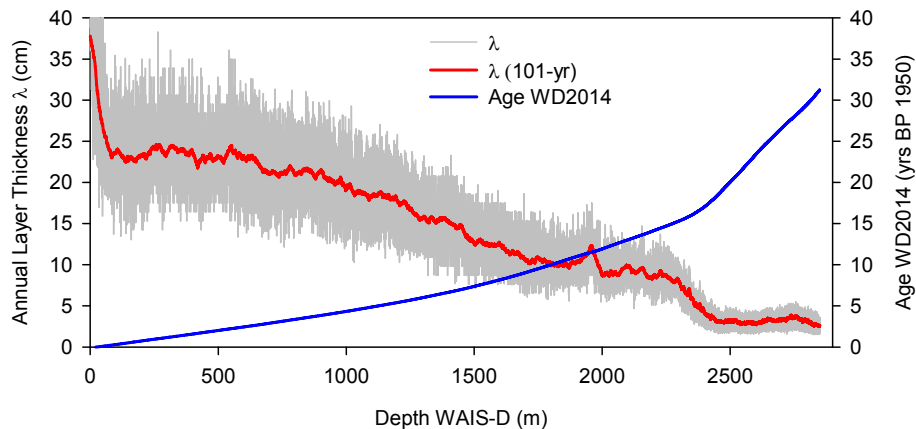


Figure 8. Depth-age profile for WAIS Divide and evolution of the annual-layer thickness (λ) for the annual-layer-dated part of the WD2014 chronology.

[Title Page](#)[Abstract](#)[Introduction](#)[Conclusions](#)[References](#)[Tables](#)[Figures](#)[Back](#)[Close](#)[Full Screen / Esc](#)[Printer-friendly Version](#)[Interactive Discussion](#)

The WAIS Divide deep ice core WD2014 chronology

M. Sigl et al.

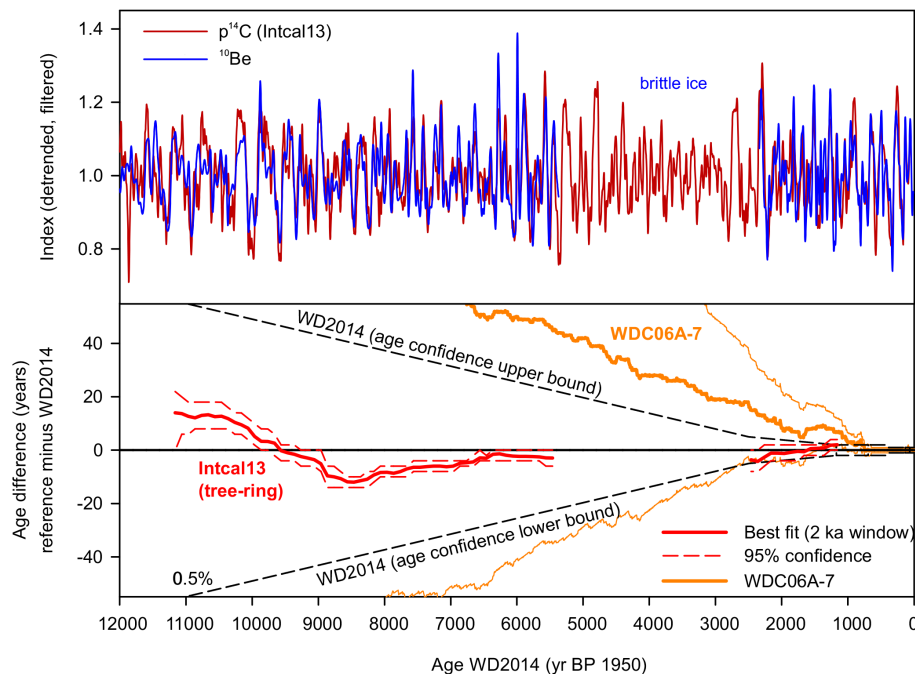


Figure 9. Comparison to the independent chronology Intcal13. (Upper panel): filtered ^{10}Be (blue) and ^{14}C (red) data on their respective timescales. (Lower panel): most likely time shift (red line) for the highly significant correlations together with the 2σ uncertainty range inferred from the r^2 distribution. Results are superimposed on a WD2014 age uncertainty envelope using an absolute age uncertainty of 0.5% over most of the Holocene. Also shown is the difference between the WAIS-Divide chronologies (WDC06A-7 minus WD2014) indicating consistent younger ages for WD2014. Ice corresponding to the age interval 2.5–5.4 ka BP has not been sampled for ^{10}Be .

[Title Page](#)
[Abstract](#)
[Introduction](#)
[Conclusions](#)
[References](#)
[Tables](#)
[Figures](#)

[Back](#)
[Close](#)
[Full Screen / Esc](#)
[Printer-friendly Version](#)
[Interactive Discussion](#)

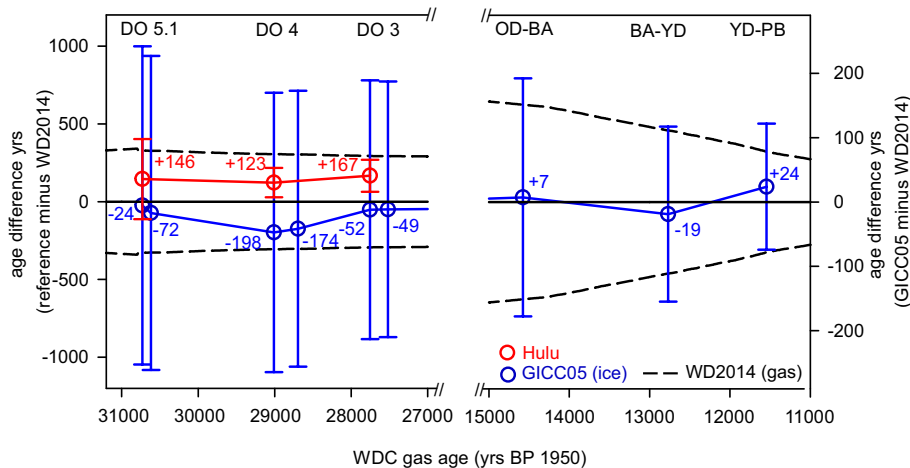



Figure 10. Comparison between WD2014 and two independently-dated records from the Northern Hemisphere. Age differences are shown between WD2014 and GICC05 (NGRIP-Project-Members, 2004) and between WD2014 and Hulu cave (Wang et al., 2001; Buizert et al., 2015; Edwards et al., in review) using CH_4 synchronization for time periods of rapid climate transition (i.e., NGRIP $\delta^{18}\text{O}$, Hulu $\delta^{18}\text{O}_{\text{calcite}}$) between 31 and 27 ka BP (left panel) and between 15 and 11 ka BP (right panel). We use a Greenland- CH_4 phasing of 50 ± 30 years for the YD/PB transition, 45 ± 30 years for the OD/BA transition and a phasing 25 ± 30 years for all other transitions (Rosen et al., 2014; Buizert et al., 2015). We assume no age difference between Hulu and CH_4 during the transition of DO 5.1, DO 4 and DO 3. Note the different scaling of the respective y axis for the two time periods. A positive value means that the reference record is older than WD2014. Error bars represent 2σ age uncertainties of the reference chronologies. Also shown are gas-age uncertainties (black dashed line) for WD2014 (Buizert et al., 2015).

Title Page

Abstract

Introduction

Conclusions

References

Tables

Figures



Back

Close

Full Screen / Esc

Printer-friendly Version

Interactive Discussion

